Hindawi
International Journal of Antennas and Propagation
Volume 2019, Article ID 6393401, 8 pages
https://doi.org/10.1155/2019/6393401

Research Article

Inscribed Fibonacci Circle Fractal in a Circular Radiator for Ultra-Wideband Antenna Operation and Size Reduction

J. A. Tirado-Mendez,[1] **D. Martinez-Lara**,[1] **H. Jardon-Aguilar**,[2] **R. Flores-Leal**,[2] **and E. A. Andrade-Gonzalez**[3]

[1]*Instituto Politécnico Nacional, SEPI-Electrical Engineering, Av. IPN S/N, Lab. EMC, 07738 Mexico City, Mexico*
[2]*CINVESTAV-IPN, Telecommunications Section, Av. IPN 2508, San Pedro Zacatenco, 07360 Mexico City, Mexico*
[3]*UAM-Azcapotzalco, Electronics Department, Communicatons Area, San Pablo 180, 02200 Mexico City, Mexico*

Correspondence should be addressed to J. A. Tirado-Mendez; jtiradom@ipn.mx

Received 16 August 2018; Revised 12 November 2018; Accepted 29 November 2018; Published 13 February 2019

Academic Editor: Shiwen Yang

In this article, a Fibonacci circle fractal is inscribed into a circular radiator in order to provide ultra-wideband behavior as well as a 50% size reduction compared to a conventional circular monopole. The third iteration of the Fibonacci series allows the antenna to obtain a steady S11 parameter over the operation bandwidth, going from 2.7 GHz to 14 GHz, an average gain around 1 dB, with a quasi-omnidirectional radiation pattern and a group delay no bigger than 1 ns, suitable for short-pulsed communications.

1. Introduction

According to FCC regulations, communications based of short pulses need ultra-wideband devices in order to fulfill the required bandwidth without introducing dispersion, which is why UWB antennas must introduce small levels of group delay over a bandwidth from 3.1 to 10.6 GHz [1]. Many efforts and technique have been stipulated to achieve these requirements, including the addition of fractal configurations with the purpose of reaching the enhancement of several antenna electric parameters. One of these techniques is the insertion of fractals in the radiator or into the ground plane. A fractal, by definition, is a self-repetitive geometry which can improve the behavior of different structures, including antennas. At the beginning, the fractal structures were added to the radiator to obtain a multiband performance, since each part of it can resonate at a different frequency, and the whole structure behavior can be seen as a resonance overlapping as explained in [2–4].

Fractals are also used to enhance other characteristics of antennas, including bettering the bandwidth [5–7] or the gain [8], even when the fractal is not introduced into the radiator but in the ground plane. Another application of using fractals in antennas is to reduce dimensions of the radiators. This phenomenon is got since the length of a fractal can be infinite, and according to this characteristic, the electric length of a radiator is increased if the fractal is employed in it. As a result, the size of the antenna is diminished [9–13] compared to a conventional structure without any fractal iteration. On the other hand, it is important to remark that the use of fractals in antennas is not limited to one kind. Combinations of two or more have shown great advantages [14] in enhancing the performance of the antenna, including combinations with specific UWB radiators like that shown in [15]. In this work, an inscribed fractal based on a Fibonacci series is etched on a circular radiator in order to increase the bandwidth, making the port matching deeper as well as to obtain a size reduction, as will be explained in the next sections.

2. Antenna Design and Simulations

In order to compare the performance of a conventional circular monopole and a circular monopole interacting with a fractal, the first one is designed by following the instructions

given in [16]; for a lower cutoff frequency of 2.5 GHz, the radiator diameter can be obtained by

$$f_L = \frac{72}{L + r + h}\text{GHz}, \quad (1)$$

where L is the radiator diameter, $r = L/2\pi$, and h is the separation between the radiator and the ground plane. Of course, there is an option where h can be zero. Following (1) considering a substrate with a dielectric permittivity of 2.2 and a thickness of 1.27 mm, the conventional circular monopole is presented in Figure 1 and fed by a 50-ohm microstrip line.

The frequency response of the conventional monopole is presented in Figure 2, where an UWB operation is obtained, going from 2.5 to 10.5 GHz, but showing a mismatching from 3.65 to 4.9 GHz.

To make the port matching deeper [17], a Fibonacci circle fractal is circumscribed into the radiator, as well as to improve the bandwidth and to get a size reduction. The Fibonacci sequence seems to appear in different structures in nature, like sunflower seeds, leafs patterns, and even human anatomy [18]. The geometry used in the radiator is derived from the Fibonacci sequence, and it is called the Fibonacci spiral. However, instead of using a spiral like the one shown in Figure 3(a), these curves are continued to complete circles. The result is shown in Figure 3(b).

Since the radiator radius was already calculated by (1), the fractal proportion was obtained taking into account the Fibonacci sequence which produces the minimum quantity of decimal digits, where the numbers of the Fibonacci series employed are 13, 21, 34, 55, 89, and 144 and this is depicted in Table 1.

From Table 1, it is noted that the radii of the fractal circles are less than the radius of the conventional circular monopole. This is another reason why fractal configurations are suitable for antenna applications, since as explained in Section 1, the use of such structures allows the antenna to be reduced, since a fractal generates a reactive load into the radiator, which gives an increment on the electric length. This increment in the electric length is compensated by reducing the physical size of the antenna. For this particular case, from Table 1, the bigger circle has a radius of 12.42 mm, compared to the conventional one, which gives a size reduction of almost 50%.

Moreover, to enhance the port matching over the entire UWB bandwidth, two other techniques were also introduced into the prototype: a bevel technique on the ground plane underneath the feeding line and the Kraus technique, where the shape of the ground plane is modified in order to avoid abrupt changes and discontinuities over the surface electric path. Figure 4 shows a comparison of the simulated S11 parameter when the fractal by itself is used into the radiator and when the fractal-Kraus technique combination is employed. Figure 5(b) shows the Kraus technique.

As observed from Figure 4, when the fractal is inscribed into the circumference of the antenna, the bandwidth increased considerably, compared to that shown in Figure 2. Moreover, the mismatching around 4 GHz, when no fractal

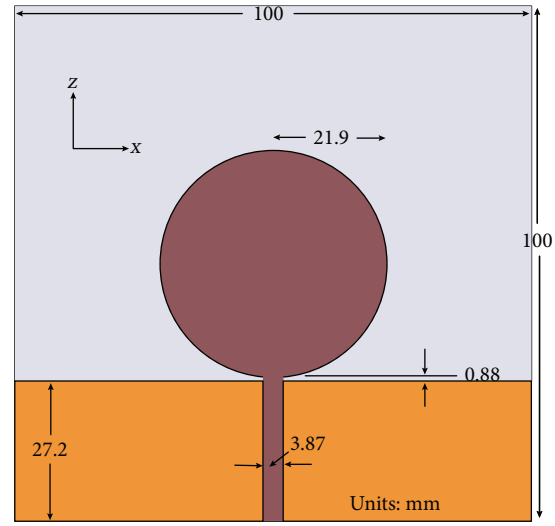

Figure 1: Conventional circular monopole with dimensions.

is used, is eliminated. Nevertheless, from Figure 4, it is also observed that close to 12 GHz, a value close to mismatching is obtained, and then, to overcome this disadvantage, the Kraus technique is also introduced, as explained above. As a result, lowering the level of the S11 parameter at the mentioned frequency is achieved. The drawback of employing the latter is that the bandwidth accomplished is reduced by almost 1 GHz compared to the results when only the fractal configuration is used.

In order to improve this behavior, the beveling technique is introduced. It has been demonstrated that this technique can be applied at lower or higher frequencies to satisfy the matching requirements by modifying the current distribution on the ground plane, making the impedance stable over certain narrow bandwidth. The shape and size of the etching below the feeding line will determine the operation frequency of the beveling [19, 20], as well as its behavior.

The proposed beveling is implemented by etching another fractal geometry composed by stepped squares. The goal of using this configuration, which has been selected after a parametric analysis was made in HFSS, is to increase the port matching at a required frequency or narrow bandwidth. In this case, it was optimized to match the port impedance at the higher cutoff frequency in order to recover the 1 GHz bandwidth lost when the Kraus technique was introduced.

Figure 5 shows the entire configuration of the circular monopole radiator, including the fractal geometry, the Kraus technique, and the beveling. The radii of each circle in Figure 5 are given in Table 1.

The simulated S11 parameter of the proposed configuration of Figure 5 is presented in Figure 6, where a great improvement compared to the conventional circular monopole is observed, but with a size reduction of 50%. The configuration makes the antenna to be coupled from 2.7 GHz to 18.8 GHz without showing any mismatching between the lower and higher cutoff frequencies.

Figure 7 shows the simulated radiation gain patterns from 3 GHz to 15 GHz.

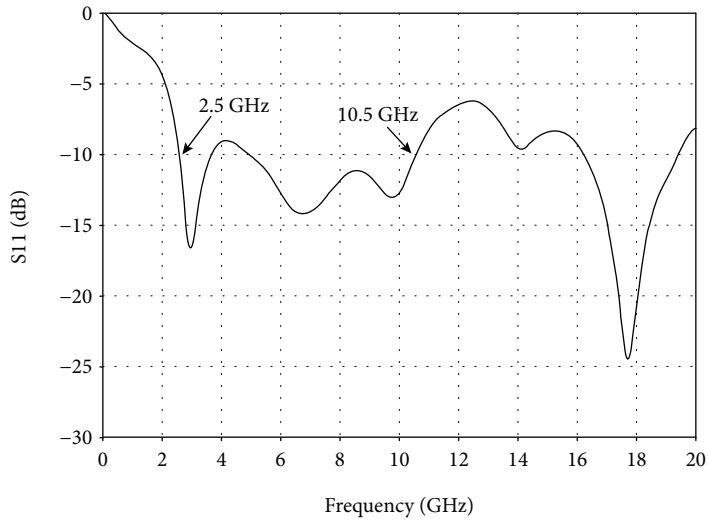

Figure 2: Simulated S11 parameter of the conventional circular monopole.

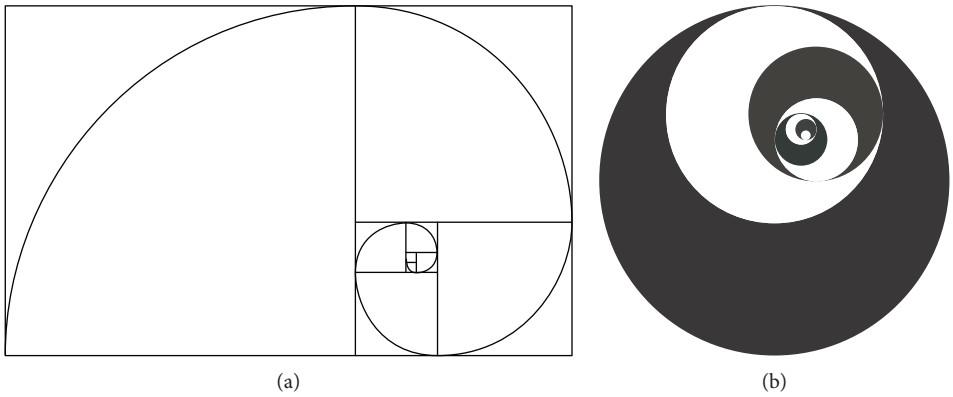

Figure 3: (a) Fibonacci spiral and (b) Fibonacci circles.

Table 1: Fibonacci series related to fractal Fibonacci circles.

Sequence value	Radius value (mm)
13	1.12125
21	1.81125
34	2.9325
55	4.74375
89	7.67625
144	12.42

As observed from Figure 7, the simulated radiation pattern behaves omnidirectional at the lower band (3 to 9 GHz); meanwhile, at higher frequencies, it behaves quasi-omnidirectional, showing some nulls around 270°.

On the other hand, to show that the antenna behaves with a small dispersion, the simulated group delay is presented in Figure 8. From this figure, it is noteworthy to remark that the antenna group delay keeps steady all over the operating bandwidth, reaching some peaks at 3.1 and 7 GHz, but not exceeding 1 ns, making it suitable for short-pulsed communications.

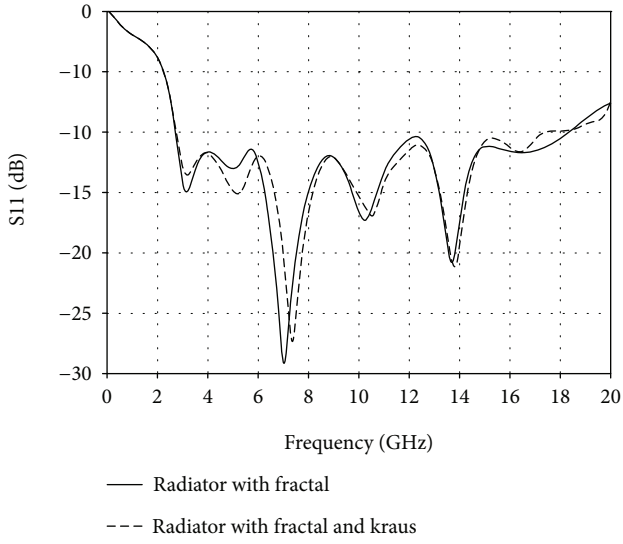

Figure 4: Simulated S11 parameter by employing the fractal and fractal-Kraus combination.

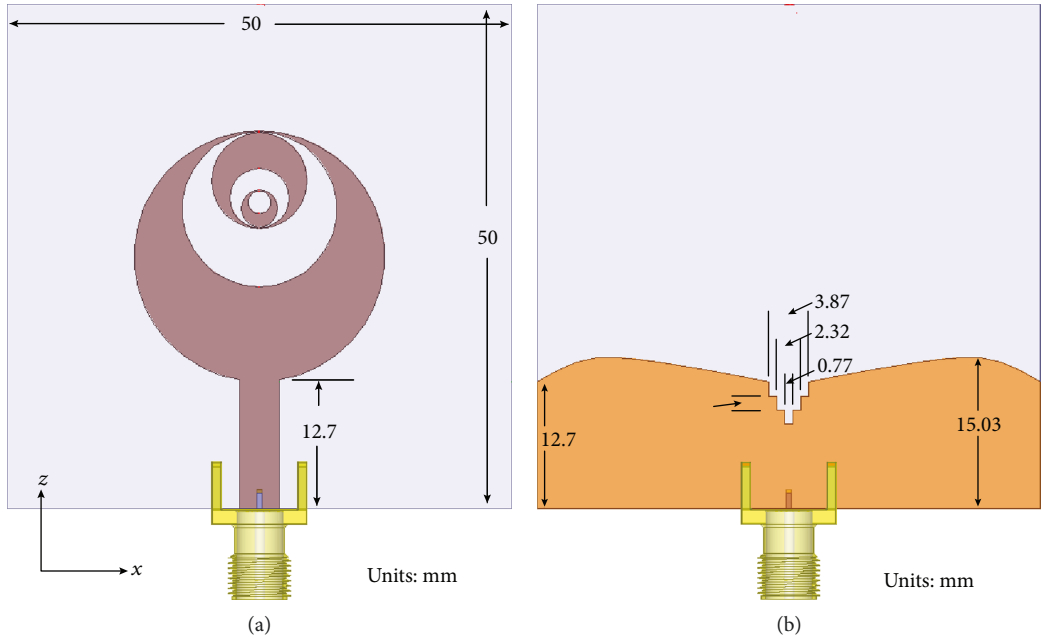

Figure 5: Proposed configuration with inscribed fractal Fibonacci circles, beveling, and Kraus technique: (a) front view and (b) back view.

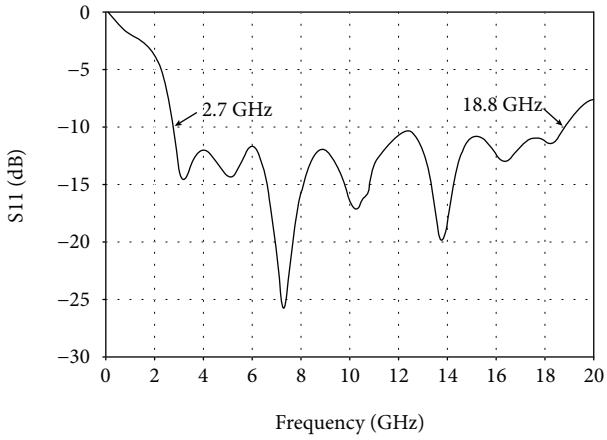

Figure 6: Simulated S11 parameter of the proposed antenna.

Once the final configuration is met, the prototype is built and characterized and results are shown below.

3. Measurements

The antenna prototype is presented in Figure 9. And the measured S11 parameter is shown in Figure 10.

According to the measured results in Figure 10, the bandwidth of the proposed antenna, for an S11 ≤ -10 dB, goes from 3.0 GHz to 14.1 GHz. Comparing the measured and simulated matching port performance clearly observed that the measured one shows a narrower bandwidth, shifting the higher cutoff frequency from 18 to 14 GHz, approximately, which is mainly due to the limitations of using a standard SMA connector at higher frequencies. Nonetheless, the antenna covers perfectly the FCC UWB bandwidth and beyond.

The measured radiation pattern is presented in Figure 11. However, due to equipment limitations in the anechoic chamber, the measurements were made up to 6 GHz. Nonetheless, as seen, the radiation pattern is quite similar to the results obtained by simulations at lower frequencies. The measured radiation pattern was done at 3, 4, 5, and 6 GHz.

As observed, the radiation pattern shows a quasi-omnidirectional characteristic at frequencies below 5 GHz; however, at 6 GHz, the out-of-roundness increases significantly, losing omnidirectionality at certain angles, where minimums are observed.

On the other hand, the measured group delay is presented in Figure 12. The maximum and minimum values are 0.78 ns and -0.160 ns, respectively, which show the antenna has a very small dispersion over the required operating bandwidth, which is ideal for shot-pulsed communications.

Finally, the comparison of the simulated and measured gain is presented in Figure 13, as well as the simulated radiation efficiency. As explained before, due to equipment limitations, the gain was measured up to 6 GHz.

At lower frequencies, where measurements could be achieved, the gain shows a convergence to the results in the simulation process, and as observed, the radiation efficiency lowers its value as the gain is decreased, going from 96 to 90%. It is also observed that there is a divergence of results for the measured and simulated gains around 5 GHz. These results were closer if a bigger mesh and a lower convergence point in the electromagnetic simulator were chosen. However, doing so requires a longer calculation time and computing resources. Authors consider that this difference can be misprized.

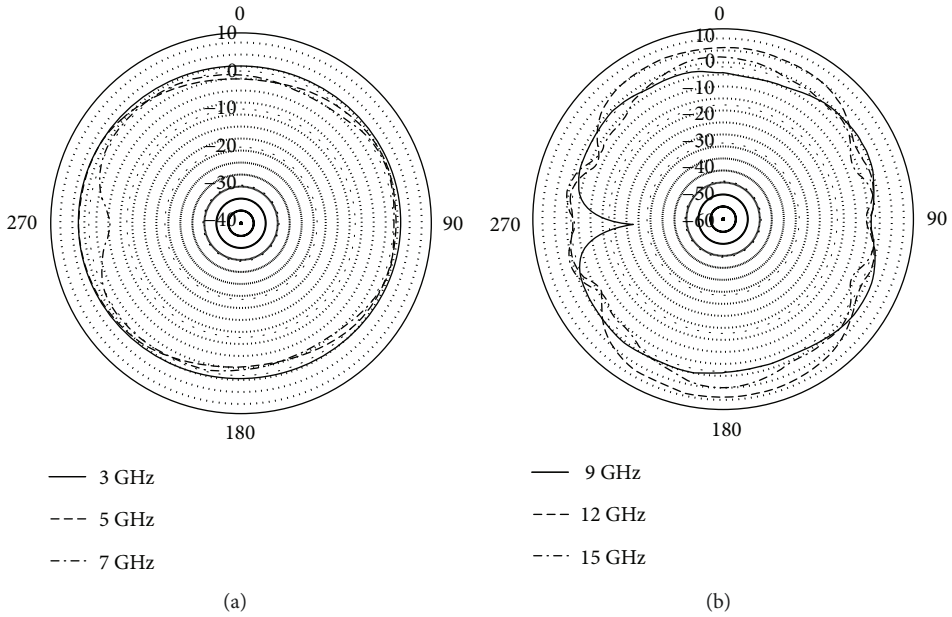

Figure 7: Simulated radiation gain patterns in the XY plane: (a) 3, 5, and 7 GHz and (b) 9, 12, and 15 GHz.

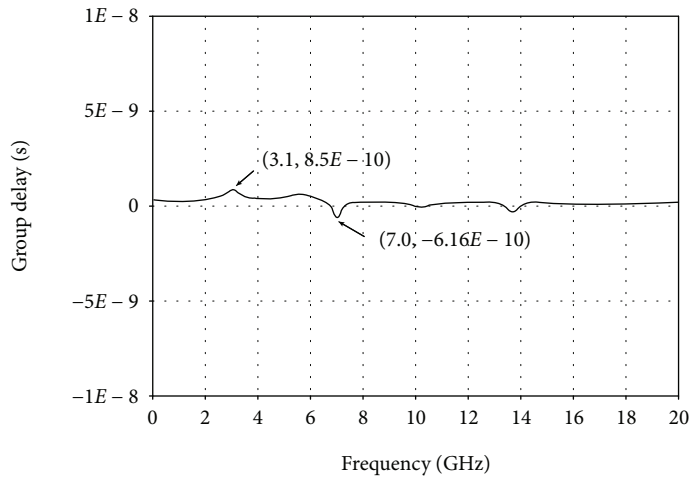

Figure 8: Simulated group delay.

Finally, a comparison of different UWB antennas is made in Table 2, taking into account bandwidth, size, and peak gain.

From Table 2, it is noted that the proposed work shows good results comparing a bandwidth-size ratio. For example, the antenna in [22], which shows a similar bandwidth, is almost twice the size of the proposed one but has bigger gain. Generally speaking, this work shows better results considering bandwidth and size, but its main drawback is the gain, which is common for monopole radiators, taking into account that the fractal antenna in this work was built in a substrate with low-value permittivity, and as it is well-known, this value plays an important role in size, gain, and radiation efficiency.

4. Analysis of Results

The use of fractals in conventional radiators improves the electric characteristics of the antenna. However, not all fractals are easy to implement, since many of them are inscribed into the radiator by an empirical way and optimized by simulations or measurements. In this paper, the fractal inscribed into the conventional circular monopole is based in a well-known theory: the Fibonacci series, making the fractal easy to implement. Moreover, since the fractal has no abrupt transitions like those shown in [3–7], to mention some cases; the current distribution over the radiator does not change dramatically, keeping the impedance in a steady state. As a result, a wider bandwidth and a stable port matching are obtained. In this case, since a standard SMA connector was employed, the bandwidth was reduced from 18 to 14 GHz, but authors affirm that using a more quality SMA connector could improve this measured result to values close to simulated ones.

On the other hand, as observed in Figure 13, the performance of the antenna is quite good, since the dispersion

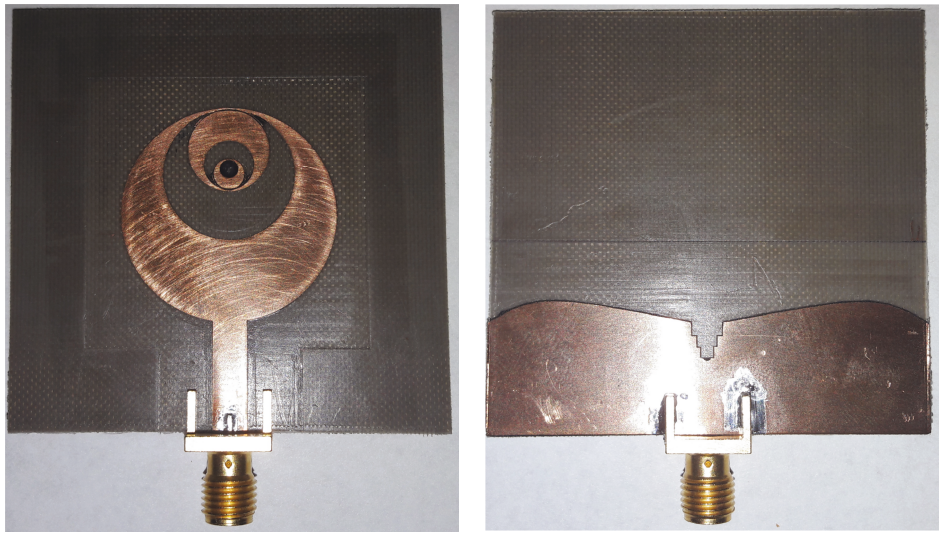

(a) (b)

Figure 9: Antenna prototype: (a) front view and (b) back view.

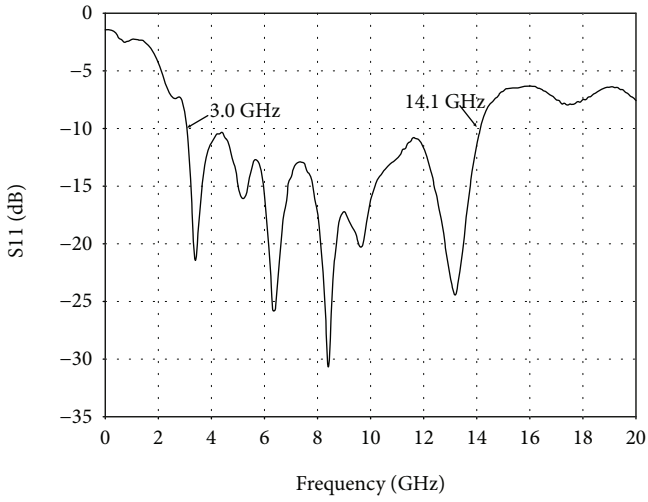

Figure 10: Measured S11 parameter of the proposed antenna.

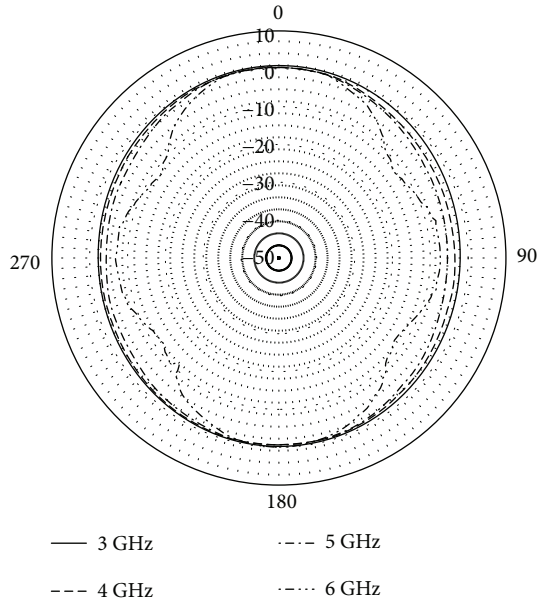

Figure 11: Measured radiation pattern on the XY plane at 3, 4, 5, and 6 GHz.

introduced by the element is very small, obtaining values below 1 ns. And finally, all these advantages are obtained with a size-reduced antenna compared to a conventional circular radiator with no fractal iteration. The area reduction reaches 50%.

5. Conclusions

Circular monopole radiators behave inherently as wideband antennas; however, there is a possibility to achieve some mismatches in the required bandwidth as observed in this previous design. To overcome this drawback, in this article, a novel Fibonacci fractal configuration was selected in order to make the antenna to perform over a wider bandwidth and to get a deeper port matching, accomplishing an UWB operation from 3 GHz to 14 GHz, approximately, but more importantly, achieving a size reduction. Moreover, to increase the port matching, other techniques were also employed: a fractal beveling technique beneath the feeding line and the Kraus technique over the ground plane. With all these combinations, the antenna presents a good behavior, obtaining a 50% size-reduced UWB antenna but paying the price of reducing the gain. In spite of this latter disadvantage, the antenna shows a very small dispersion which lets the radiator to be employed in short-pulse communications.

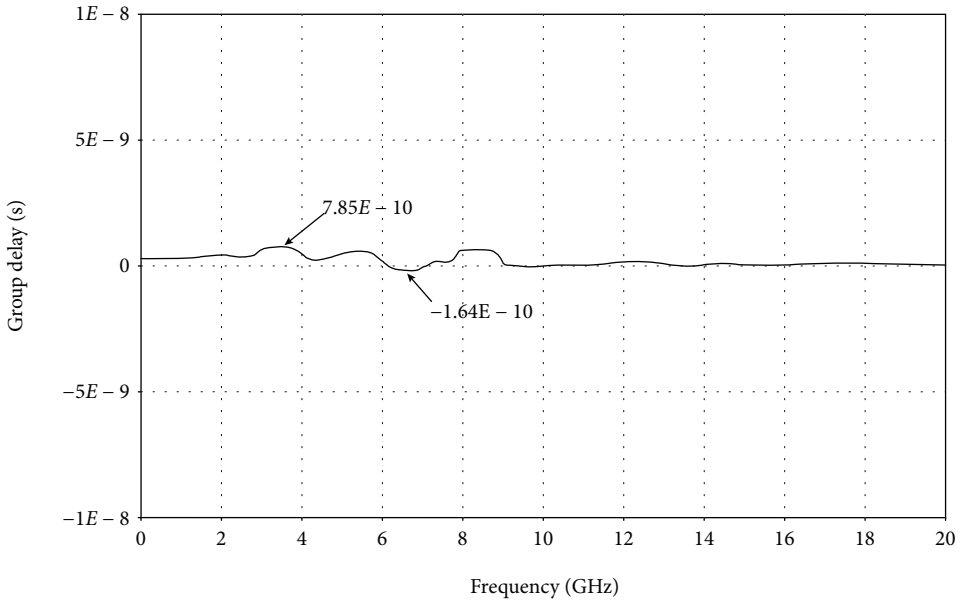

Figure 12: Measured group delay.

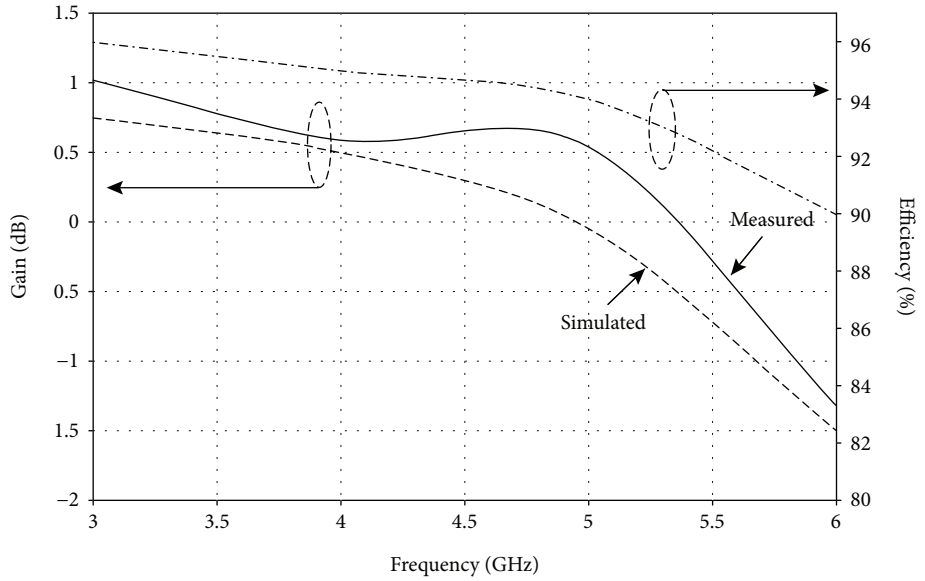

Figure 13: Comparison of simulated and measured peak gain and radiation efficiency.

Table 2: Comparison of different UWB antennas.

Reference	Bandwidth (GHz)	Antenna footprint (mm^2)	Peak gain variation (dB)
This work	3.0–14.1	50×50 ($\varepsilon_r = 2.2$)	-1.3 to 1
[21]	3–11.2	24×22 ($\varepsilon_r = 4.6$)	-2 to 5.2
[22]	2.85–15.12	85×85 ($\varepsilon_r = 4.4$)	4.5 to 6.5
[23]	2.21–11.5	42×48 ($\varepsilon_r = 4.32$)	3.6 to 7.6
[24]	2–3.12 and 4.5–5.77	50×50 ($\varepsilon_r = 4.4$)	6.74 to 7.1
[25]	3.2–10.8	90×107 ($\varepsilon_r = 2.94$)	0.5 to 4
[26]	2.43–3.26 and 6.05–15.03	20×20 ($\varepsilon_r = 4.4$)	Not defined

Data Availability

The data used to support the findings of this study are included in the article.

Conflicts of Interest

The authors declare that they have no conflicts of interest.

Acknowledgments

This work was supported by the Instituto Politécnico Nacional (project SIP-IPN 20180161).

References

[1] Federal Communications Commission, "First report and order, revision of part 15 of the commission's rules regarding ultra-wideband transmission systems," 2002, FCC 02–48.

[2] S. Kuzu and N. Akcam, "Array antenna using defected ground structure shaped with fractal form generated by Apollonius circle," *IEEE Antennas and Wireless Propagation Letters*, vol. 16, pp. 1020–1023, 2017.

[3] W.-C. Weng and C.-L. Hung, "An H-fractal antenna for multiband applications," *IEEE Antennas and Wireless Propagation Letters*, vol. 13, pp. 1705–1708, 2014.

[4] B. Hephzibah Lincy, A. Srinivasan, and B. Rajalakshmi, "Wideband fractal microstrip antenna for wireless application," in *2013 IEEE Conference on Information & Communication Technologies*, pp. 735–738, Thuckalay, Tamil Nadu, India, April 2013.

[5] S. Tripathi, S. Yadav, and A. Mohan, "Hexagonal fractal ultra-wideband antenna using Koch geometry with bandwidth enhancement," *IET Microwaves, Antennas & Propagation*, vol. 8, no. 15, pp. 1445–1450, 2014.

[6] Y. K. Choukiker and S. K. Behera, "Wideband frequency reconfigurable Koch snowflake fractal antenna," *IET Microwaves, Antennas & Propagation*, vol. 11, no. 2, pp. 203–208, 2017.

[7] A. Karmakar, R. Ghatak, and D. R. Poddar, "Inscribed gasket fractal circular monopole antenna for UWB application," in *2012 1st International Conference on Emerging Technology Trends in Electronics, Communication and Networking*, pp. 1–4, Gujarat, India, 2011.

[8] L.-R. Zhong, G.-M. Yang, and Y.-W. Zhong, "Gain enhancement of bow-tie antenna using fractal wideband artificial magnetic conductor ground," *Electronics Letters*, vol. 51, no. 4, pp. 315–317, 2015.

[9] F. Wang, F. Bin, Q. Sun, J. Fan, and H. Ye, "A compact UHF antenna based on complementary fractal technique," *IEEE Access*, vol. 5, pp. 21118–21125, 2017.

[10] A. Gorai, M. Pal, and R. Ghatak, "A compact fractal-shaped antenna for ultrawideband and bluetooth wireless systems with WLAN rejection functionality," *IEEE Antennas and Wireless Propagation Letters*, vol. 16, pp. 2163–2166, 2017.

[11] S. Singhal and A. K. Singh, "CPW-fed hexagonal Sierpinski super wideband fractal antenna," *IET Microwaves, Antennas & Propagation*, vol. 10, no. 15, pp. 1701–1707, 2016.

[12] L. Albasha, M. Ali, M. Taghadosi, and N. Qaddoumi, "Miniaturised printed elliptical nested fractal multiband antenna for energy harvesting applications," *IET Microwaves, Antennas & Propagation*, vol. 9, no. 10, pp. 1045–1053, 2015.

[13] H. Soleimani and H. Orazi, "Miniaturisation of the triangular patch antenna by the novel dual-reverse-arrow fractal," *IET Microwaves, Antennas & Propagation*, vol. 9, no. 7, pp. 627–633, 2015.

[14] D. V. Kiran, D. Sankaranarayanan, and B. Mukherjee, "Compact embedded dual-element rectangular dielectric resonator antenna combining Sierpinski and Minkowski fractals," *IEEE Transactions on Components, Packaging and Manufacturing Technology*, vol. 7, no. 5, pp. 786–791, 2017.

[15] B. Biswas, R. Ghatak, and D. R. Poddar, "A fern fractal leaf inspired wideband antipodal Vivaldi antenna for microwave imaging system," *IEEE Transactions on Antennas and Propagation*, vol. 65, no. 11, pp. 6126–6129, 2017.

[16] C.-Y.-D. Sim, W.-T. Chung, and C.-H. Lee, "A circular-disc monopole antenna with band-rejection function for ultrawideband application," *Microwave and Optical Technology Letters*, vol. 51, no. 6, pp. 1607–1613, 2009.

[17] R. Leyva-Hernandez, J. A. Tirado-Mendez, H. Jardon-Aguilar, R. Flores-Leal, and R. Linares Y Miranda, "Reduced size elliptic UWB antenna with inscribed third iteration sierpinski triangle for on-body applications," *Microwave and Optical Technology Letters*, vol. 59, no. 3, pp. 635–641, 2017.

[18] E. Maor and E. Jost, *Beautiful Geometry*, Princeton University Press, New Jersey, USA, 2014.

[19] E. Gomez-Nuñez, H. Jardon-Aguilar, J. A. Tirado-Mendez, and R. Flores-Leal, "Ultra-wideband slotted disc antenna compatible with cognitive radio applications," *Progress In Electromagnetics Research Letters*, vol. 34, pp. 53–63, 2012.

[20] M. A. Peyrot-Solis, G. M. Galvan-Tejada, and H. Jardon-Aguilar, "State of the art in ultra-wideband antennas," in *IEEE, 2nd International Conference on Electrical and Electronics Engineering (ICEEE) and XI Conference on Electrical Engineering (CIE 2005)*, pp. 101–105, Mexico City, Mexico, September 2005.

[21] R. Azim, M. T. Islam, and N. Misran, "Compact tapered-shape slot antenna for UWB applications," *IEEE Antennas and Wireless Propagation Letters*, vol. 10, pp. 1190–1193, 2011.

[22] A. Dastranj and H. Abiri, "Bandwidth enhancement of printed E shaped slot antennas fed by CPW and microstrip line," *IEEE Transactions on Antennas and Propagation*, vol. 58, no. 4, pp. 1402–1407, 2010.

[23] D. Abed, S. Redadaa, and H. Kimouche, "Printed ultra-wideband stepped-circular slot antenna with different tuning stubs," *Journal of Electromagnetic Waves and Applications*, vol. 27, no. 7, pp. 846–855, 2013.

[24] S. Pimpol and R. Wongsan, "CPW-fed dual wideband using stub split-ring rectangular slot antenna," *2013 10th International Conference on Electrical Engineering/Electronics, Computer, Telecommunication and Information Technology*, 2013, pp. 1–4, Thailand, Krabi, Krabi, Thailand, May 2013.

[25] X. D. Huang, C. H. Cheng, and L. Zhu, "An ultrawideband (UWB) slotline antenna under multiple-mode resonance," *IEEE Transactions on Antennas and Propagation*, vol. 60, no. 1, pp. 385–389, 2012.

[26] M. Ojaroudi and N. Ojaroudi, "Low profile slot antenna with dual band-notched function for UWB systems," *Microwave and Optical Technology Letters*, vol. 55, no. 5, pp. 951–954, 2013.